British Journal of Pharmacology (2005) 145, 1017–1026
www.nature.com/bjp

Caveolin-1 gene knockout impairs nitrergic function in mouse small intestine

[1]Ahmed F. El-Yazbi, [1]Woo-Jung Cho, [1]Geoffrey Boddy & *,[1]Edwin E. Daniel

[1]Department of Pharmacology, Faculty of Medicine and Dentistry, University of Alberta, 9-10 Medical Sciences Bldg., Edmonton, AB, Canada T6G 2H7

1 Caveolin-1 is a plasma membrane-associated protein that is responsible for caveolae formation. It plays an important role in the regulation of the function of different signaling molecules, among which are the different isoforms of nitric oxide synthase (NOS).

2 Nitric oxide (NO) is known to be an important inhibitory mediator in the mouse gut. Caveolin-1 knockout mice ($Cav1^{-/-}$) were used to examine the effect of caveolin-1 absence on the NO function in the mouse small intestine (ileum and jejunum) compared to their genetic controls and BALB/c controls.

3 Immunohistochemical staining showed loss of caveolin-1 and NOS in the jejunal smooth muscles and myenteric plexus interstitial cells of Cajal (ICC) of $Cav1^{-/-}$ mice; however, nNOS immunoreactive nerves were still present in myenteric ganglia.

4 Under nonadrenergic noncholinergic (NANC) conditions, small intestinal tissues from $Cav1^{-/-}$ mice relaxed to electrical field stimulation (EFS), as did tissues from control mice. Relaxation of tissues from control mice was markedly reduced by *N*-omega-nitro-L-arginine (10^{-4} M), but relaxation of $Cav1^{-/-}$ animals was affected much less. Also, $Cav1^{-/-}$ mice tissues showed reduced relaxation responses to sodium nitroprusside (100 μM) compared to controls; yet there were no significant differences in the relaxation responses to 8-bromoguanosine-3′ : 5′-cyclic monophosphate (100 μM).

5 Apamin (10^{-6} M) significantly reduced relaxations to EFS in NANC conditions in $Cav1^{-/-}$ mice, but not in controls.

6 The data from this study suggest that caveolin-1 gene knockout causes alterations in the smooth muscles and the ICC, leading to an impaired NO function in the mouse small intestine that could possibly be compensated by apamin-sensitive inhibitory mediators.
British Journal of Pharmacology (2005) **145,** 1017–1026. doi:10.1038/sj.bjp.0706289;
published online 6 June 2005

Keywords: Caveolin-1 knockout; nitric oxide; mouse small intestine; nitric oxide synthase; interstitial cells of Cajal; apamin

Abbreviations: ATP, adenosine-5′-triphosphate; BCGMP, 8-bromoguanosine-3′ : 5′-cyclic monophosphate; $Cav1^{-/-}$, caveolin-1 knockout mice; $Cav1^{+/+}$, caveolin-1 knockouts genetic controls; cGMP, cyclic guanosine monophosphate; EFS, electric field stimulation; HuC/D, human HuC/HuD protein; ICC, interstitial cells of Cajal; LNNA, *N*-omega-nitro-L-arginine; NANC, nonadrenergic noncholinergic; nNOS-C, nNOS with C-terminal epitope; nNOS-N, nNOS with N-terminal epitope; PACAP, pituitary adenylate cyclase-activating peptide; PB, phosphate buffer; PBS, phosphate buffered saline; SNP, sodium nitroprusside; TX-100, Triton X-100; VIP, vasoactive intestinal peptide

Introduction

Caveolins are 21–24 kDa integral membrane proteins that have been identified as principal components of caveolar membranes *in vivo* (Rothberg *et al*., 1992; Chang *et al*., 1994). Caveolins insert into the inner leaflet of plasma membrane in the form of homo-oligomers to form the characteristic flask-shaped caveolae (Sargiacomo *et al*., 1995). Caveolin-1 is essential for caveolae formation in adipocytes, endothelial cells, pneumocytes, fibroblasts, and smooth muscles (Scherer *et al*., 1994; Tang *et al*., 1996). Full-length caveolin-1 contains three domains: a 101-residue N-terminal domain, a 33-residue membrane spanning region, and a 44-residue C-terminal domain (Scherer *et al*., 1995). A 20-aminoacyl residue domain (residues 82–101), the caveolin scaffolding domain, recognizes a caveolin-binding motif in proteins interacting with caveolin-1. The caveolin scaffolding domain and its consensus sequence are absolutely conserved from chicken to human (Couet *et al*., 1997). Among the signaling molecules that contain the caveolin-binding motif are heterotrimeric G-proteins, H-Ras, Src family tyrosine kinases, protein kinase C isoforms, and nitric oxide synthase (NOS) isoforms (Engleman *et al*., 1998; Okamoto *et al*., 1998; Smart *et al*., 1999; Felly-Bosco *et al*., 2000; Sato *et al*., 2004).

The binding and interaction between caveolin-1 and NOS has been extensively studied in the endothelium (Garcia-Cardena *et al*., 1996a; 1997; Ju *et al*., 1997). *In vitro* interaction between caveolin-1 and endothelial NOS (eNOS) inhibits eNOS activity (Ju *et al*., 1997). Moreover, eNOS is directly targeted to the caveolar domains of the plasma membrane *via* post-transcriptional palmitoylation (Garcia-Cardena *et al*.,

*Author for correspondence; E-mail: edaniel@ualberta.ca

1996b). *In vivo* studies have also shown that caveolin-1 is an important negative modulator of eNOS (Bucci *et al*., 2000). However, it has been shown that the stimulated production of NO becomes optimal only when eNOS is correctly targeted into the caveolae. That is because the mutation that blocked the N-terminal palmitoylation of eNOS and its subsequent targeting to the caveolae has led to the prevention of NO release upon stimulation (Feron *et al*., 1996). In addition, different studies have examined the interaction between caveolin-1 and other NOS isoforms (Garcia-Cardena *et al*., 1997; Michel *et al*., 1997; Venema *et al*., 1997; Salapatek *et al*., 1998a; Segal *et al*., 1999; Felly-Bosco *et al*., 2000; Cho & Daniel, 2005). Binding to caveolin-1 has been shown to inhibit NO production in neuronal NOS (nNOS) (Venema *et al*., 1997) and inducible NOS (iNOS) (Felly-Bosco *et al*., 2000).

In mouse intestine, studies in our laboratory have shown that the disruption of caveolae and caveolin-1 in the smooth muscles and interstitial cells of Cajal (ICC) with methyl-β-cyclodextrin reduced pacing frequencies and inhibited paced contractions (Daniel *et al*., 2004). This suggests the importance of caveolin-1 and caveolae in the control of mouse gut motility. In addition, co-localization between caveolin-1 and myogenic NOS, a splice variant of nNOS (Huber *et al*., 1998), was shown in smooth muscles and ICC in the jejunum and lower esophageal sphincter of wild-type mice (Cho & Daniel, 2005). This supports a possible role for caveolin-1 in the regulation of nNOS activity in the murine small intestine. However, disruption of caveolin-1 and caveolae did not appear to affect cholinergic innervation to the mouse intestine (Daniel *et al*., 2004).

Caveolin-1 knockout mice (Cav1) lack morphologically identifiable caveolae in tissues known to express caveolin-1 (Razani *et al*., 2002). Cav1 show a number of abnormalities: defects in caveolar endocytosis, lung hypercellularity, decreased vascular tone, and atrophic fat pads (Razani *et al*., 2002). In addition, caveolin-1 null cells and tissues exhibit behaviors different from wild-type ones, showing defects in the sorting of glycosyl phosphatidyl inositol (GPI)-anchored and lipid-modified proteins (Sotgia *et al*., 2002). Studies of isolated aortic rings from Cav1 suggested that, in these tissues, eNOS retains a higher level of activity because caveolin-1, being one of the regulatory component of eNOS action, is lacking (Drab *et al*., 2001; Razani *et al*., 2001).

To date, no data are available to describe the effects of caveolin-1 gene knockout on the NO function in mouse intestine, where NO is involved as an inhibitory neurotransmitter in all regions of the gut (Okasora *et al*., 1986; Satoh *et al*., 1999), where the use of NOS inhibitors affects the inhibitory mechanisms (Lyster *et al*, 1995; Spencer *et al*., 1998a). Changes in NO function have a strong impact on mechanical and electrical patterns in various gut preparations (Azzena & Mancinelli, 1999; Mulè *et al*., 1999; Serio *et al*., 2001; Mulè & Serio, 2002). Therefore, our aim in the present study is to examine the effects of caveolin-1 gene knockout on NO function in mouse small intestine.

Methods

All animal experiments were conducted according to a laboratory animal protocol approved by our University Animal Policy and Welfare Committee.

Functional studies

Preparation of tissue Male 6–8-weeks-old caveolin-1 knockout [(cav<tm 1 M Is>/J) ($Cav1^{-/-}$)], and control [(B6 129 SF2/J) ($Cav1^{+/+}$) and BALB/c] mice (Jackson laboratory, Bar Harbor, Maine, U.S.A.) were killed by cervical dislocation. After opening of the abdominal wall, the digestive tract, beginning from the level of the stomach to the rectum, was removed from the mouse and immediately placed into a beaker of Krebs–Ringer solution containing (in mM): 115.5 NaCl, 21.9 $NaHCO_3$, 11.1 D-glucose, 4.6 KCl, 1.16 $MgSO_4$, 1.16 NaH_2PO_4, and 2.5 $CaCl_2$, at room temperature (21–22°C), and pre-equilibrated with carbogen (95% O_2 and 5% CO_2). In a dissection dish, filled with Krebs–Ringer solution and continuously bubbled with carbogen, small intestinal tissue (ileum and jejunum) was isolated and cut into 1–1.5 cm segments. The intestinal content, if any, was pushed out by gently rubbing the segments with dissection forceps. To study the longitudinal muscle contractions, the tissue segments were placed between two platinum concentric circular electrodes. Each segment was tied to a hook at the bottom of the electrode holder by a silk suture thread and the top of the tissue was also tied with thread and attached to a strain gauge (Grass FT-03). The muscle preparations were placed into muscle baths, filled with 10 ml Krebs–Ringer solution, bubbled continuously through the experiment with carbogen, and maintained at a temperature of 37°C. The tissue was subjected to a slight tension, just enough to obtain the maximum amplitude of spontaneous, phasic activity. Tissue contractile activities were recorded on a Grass Model 7D Polygraph.

Experimental protocols Nonadrenergic noncholinergic (NANC) conditions were achieved by equilibrating in atropine (10^{-7} M), timolol (10^{-6} M), and prazosin (10^{-6} M) for 20 min. Electrical field stimulation (EFS) for 10 s (parameters: 50 V cm^{-1} and 0.5 ms) was carried out at 1, 3, 10, and 30 pulses per second (pps), with a 10-min interval between each series. At the end of each experiment, all tissues were washed twice with 10 ml Ca^{2+}-free Krebs with 1.0 mM EGTA. This relaxed the tissues to basal passive tensions and abolished spontaneous contractions.

Experimental procedures In some experiments, *N*-omega-nitro-L-arginine (LNNA) at 100 μM was added to the tissue bath following an EFS cycle at the four frequencies. A 20-min incubation period was allowed, followed by another EFS cycle at all frequencies. The inhibitory responses to EFS after LNNA were compared to those before LNNA. Apamin, 1 μM, was added initially in some experiments and allowed a 20-min incubation period with the tissue, followed by a cycle of EFS at all frequencies. Pilot experiments with apamin showed that clearer and more consistent results were obtained when apamin was added before the first cycle of EFS. In these experiments, the results were compared to time controls in which the tissues were not pretreated with apamin. In some of the apamin experiments (in $Cav1^{-/-}$ tissues), LNNA was added after the first cycle of EFS and allowed a 20-min incubation period, followed by another cycle of EFS at all frequencies. These experiments were carried out in order to examine the effect of the combination of LNNA and apamin on EFS-induced relaxation.

The effects of sodium nitroprusside (SNP) at 100 μM were also evaluated, where SNP was added directly after the equilibration period and the inhibitory effects were measured when the relaxation to SNP was maximal. The SNP dose lies at the just submaximal range. This dose was chosen as it gave the clearest and most consistent responses and repetitive dosing appeared to produce tachyphylaxis. Similarly, in some experiments, 8-bromoguanosine-3′ : 5′-cyclic monophosphate (BCGMP) at 100 μM was added directly after the equilibration period. Due to the relatively slow permeability of BCGMP, its inhibitory effect was measured after 5 min. The BCGMP dose, being in the submaximal range, was chosen so that a clear and consistent response was obtained. In preliminary experiments, repeated doses appeared to decrease in effect.

All the drugs used for functional experiments, with the exception of apamin, were dissolved in double-distilled water. Apamin was dissolved in 0.05 M acetic acid. Acetic acid (0.05 M) alone, in the amount added (10 μl 10 ml^{-1}), did not appear to affect the functional activity of the tissue.

Data analysis Amplitudes of the spontaneous contractions and the inhibitory phases were measured as the values above the passive tension determined at the end of the experiments. They were measured as the mean of individual contractions over at least 15 contractions. Inhibitions in response to EFS, SNP, and BCGMP were calculated by normalizing the amplitude in the inhibitory phase to the amplitude of the muscle activity directly precedent to the inhibitory stimulus (taken as 100%). The measurements were entered into GraphPad Instat and statistically tested using analysis of variance (ANOVA) with Bonferroni *post hoc* test ($P<0.05$ considered to be statistically significant). The *n*-values represent the number of mice whose small intestine provided segments for study.

Ultrastructural study

The jejunal tissue of BALB/c and Cav1$^{-/-}$ mice was pre-fixed in a mixed fixative as described previously (Daniel *et al*., 2004) for 2 h at 4°C. The tissue was washed in 0.075 M sodium cacodylate buffer overnight at 4°C. The tissue was dissected to prepare a size of $1.0\times4.0\,mm^2$ and muscular layers were separated from mucosa layers. The tissue was *en bloc* stained in saturated (1%) uranyl acetate in 70% ethanol for 1 h at room temperature, post-fixed in 1% OsO_4 in 0.05 M sodium cacodylate buffer (pH 7.4) for 2 h at 4°C, dehydrated in graded ethanol and propylenoxide, and embedded in TAAB 812 resin. Ultra-thin sections were cut, mounted on 100- or 300-mesh grids coated with 0.25% formvar solution in ethylene dichloride, and stained with 13% uranyl acetate in 50% ethanol and lead citrate. The grids were examined in a Philips 410 electron microscope equipped with a charge-coupled device camera (MegView III) at 80 kV.

Immunohistochemical studies

Cryosections Jejunal tissues from three Cav1$^{-/-}$ mice were prepared as cryosections. The tissues were opened along the mesenteric border and pinned on a petri dish of Sylgard silicon rubber filled with oxygenated ice-cold Krebs–Ringer's solution. The tissues were fixed in ice-cold 4% paraformaldehyde in 0.1 M sodium phosphate buffer (PB; pH 7.4) for 4 h at room temperature, cryoprotected in 30% sucrose in PB including 0.1 NaN_3 overnight at 4°C, and then stored at −80°C until used. Cryosections of 10 μm thickness were obtained using a cryostat (Leitz 1720 digital cryostat, Germany). The cryosections were attached to a slide glass coated with 2% 3-aminopropyl-triethoxysilane in acetone, and were dried overnight at 4°C. The dried cryosections were used for double immunohistochemistry.

Whole-mount preparations Jejunal tissues from five Cav1$^{-/-}$ and five Cav1$^{+/+}$ mice were prepared as whole-mount preparations. The tissues were opened along the mesenteric border, stretched, and pinned on a petri dish of Sylgard silicon rubber filled with oxygenated ice-cold Krebs–Ringer's solution. The tissues were fixed in the same fixative used for cryosections for 4 h at room temperature. The fixed tissues were washed in ice-cold phosphate-buffered saline (PBS; 0.85 NaCl in 0.01 M sodium PB, pH 7.0) eight times (once every 30 min), dehydrated in dimethylsulfoxide (DMSO) three times (once every 10 min), rehydrated in PBS three times (once every 15 min), and stored in 30% sucrose in PBS including 0.1% NaN_3 at 4°C. The fixed tissues were cut to make specimens of $1.0\times1.5\,cm^2$ (circular muscle layer × longitudinal muscle layer) by a dissection knife. In each specimen, muscular layers (circular and longitudinal muscle layers) were separated from the mucosa layers (mucosa and submucosa layers). To obtain myenteric plexus attached to longitudinal muscle layer, the circular muscle fibers were peeled away by tweezers. All micro-dissections were carried out under a dissection microscope and the separated specimens were used for double immunohistochemistry.

Double immunohistochemical staining using cryosections The cryosections were washed in 0.3% Triton X-100 (TX-100) in PBS three times (once every 15 min). The cryosections were incubated in 10% normal donkey serum to reduce nonspecific binding for 1 h at room temperature. *Primary antibodies*: Mouse anti-caveolin-1, guinea-pig anti-rat nNOS with COOH-terminal epitope (nNOS-C), and rabbit anti-rat nNOS with NH_2-terminal epitope (nNOS-N) were incubated for 19–20 h at 4°C or room temperature. The cryosections were washed in 0.3% TX-100 in PBS three times (once every 15 min) and then incubated in secondary antibodies, Cy3-conjugated donkey anti-mouse IgG, FITC-conjugated donkey anti-guinea-pig IgG, and Alexa Fluor® 488-conjugated goat anti-rabbit IgG for 1 h at room temperature. The cryosections were washed in 0.3% TX-100 in PBS twice (separated by 15 min) and then washed in PBS without TX-100 once after 15 min. The cryosections were mounted with aqua-mount medium with antifading agents.

Immunohistochemical staining using whole-mount preparations To improve antibody penetration, the separated specimens were incubated in PBS including 0.5% TX-100 in PBS for 1 h at room temperature. The specimens were incubated in normal serum (10% normal goat serum of the final incubation volume) or mixed normal sera (10% normal goat serum and 10% normal donkey serum of the final incubation volume) in 0.5% TX-100 in PBS for 1 or 2 h at room temperature to reduce nonspecific binding proteins. The rabbit anti-rat nNOS with NH_2-terminal epitope was used at a concentration of 1 : 100, the mouse anti-HuC/HuD neural

protein (HuC/D) was used at a concentration of 1 : 200, and the rabbit anti-vimentin was used undiluted. The specimens were incubated in the rabbit anti-vimentin or mixed primary antibodies (rabbit anti-nNOS and mouse anti-HuC/D) in 0.5% TX-100 in PBS into a 24-well tissue culture plate for three nights at 4°C. The specimens were washed in 0.5% TX-100 in PBS three times (once every 15 min) and then incubated for 3 h at room temperature with Alexa Fluor® 488-conjugated goat anti-rabbit IgG or mixed secondary antibodies: Alexa Fluor® 488-conjugated goat anti-rabbit IgG and Alexa Fluor® 405-conjugated goat anti-mouse IgG. The specimens were washed in 0.5% TX-100 in PBS twice (separated by 15 min), washed in PBS once after 15 min, and then mounted with aqua-mount medium. All primary antibodies were reconstituted in distilled water according to the reconstitution protocol from the maker.

To determine the specificity of immunostaining of cryosections and whole-mount preparations, primary antibodies were omitted.

Confocal images The immunofluorescent-labeled cryosections and whole-mount preparations were observed by confocal laser-scanning microscope (CLSM 1500, Zeiss Co., Germany) with one- or two-photon lasers. In whole-mount preparations, HuC/D-immunoreactive cells, labeled with Alexa Fluor® 405, were originally blue. However, the blue was converted to red to show yellow colour upon co-localization with nNOS-N-immunoreactive cells labeled with Alexa Fluor® 488 (green). The resolution of the confocal images obtained from cryosections and whole-mount preparations was originally 512×512 pixels, and then the images were edited and enhanced by LSM 5 and Adobe PhotoShop software.

Morphometric study nNOS-N-immunoreactive (nNOS-N-IR) cells and HuC/D-immunoreactive (HuC/D-IR) cells in myenteric ganglia were counted independently by two persons (WJC and EED) to be analyzed statistically (contingency analysis). Only nNOS-N-IR cells with immunostaining in their cytoplasm brighter than glial cells and background staining were counted.

Materials

Atropine, timolol (as maleate salt), prazosin hydrochloride, LNNA, SNP, BCGMP, and apamin were purchased from Sigma (Oakville, ON, Canada). Apamin was dissolved in 0.05 M acetic acid. Tweezers were purchased from WPI Inc. (FL, U.S.A.). The mouse anti-caveolin-1 was from BD Biosciences (U.S.A.). The guinea-pig anti-rat nNOS with COOH-terminal epitope and the rabbit anti-rat nNOS with NH_2-terminal epitope were from Euro-Diagnostica (Malmö, Sweden). The mouse anti-HuC/HuD neural protein, Alexa Fluor® 488 goat anti-rabbit IgG, and Alexa Fluor® 405 goat anti-mouse IgG were from Molecular Probe (OR, U.S.A.). The rabbit anti-vimentin was from Abcam, Inc. (MA, U.S.A.). Cy3-conjugated donkey anti-guinea-pig IgG and Cy3-conjugated donkey anti-mouse IgG were from Jackson Immuno Research Laboratories, Inc. (PA, U.S.A.). FITC-conjugated donkey anti-guinea-pig IgG was from Research Diagnostics, Inc. (NJ, U.S.A.). Uranyl acetate, OsO_4, and TAAB 812 resin were purchased from Marivac, Inc. (Montreal, Quebec, Canada). Lead acetate was purchased from TAAB Lab. (Aldermaston, U.K.). Mesh grids and formvar solution in ethylene dichloride were purchased from Electron Microscopy Sciences (PA, U.S.A.). DMSO was purchased from Caledon Laboratories Ltd (ON, Canada). 3-aminopropyltriethoxysilane was purchased from Sigma (St Louis, MO, U.S.A.). Tissue culture plates were purchased from ICN Biomedicals, Inc. (OH, U.S.A.). Aqua-mount medium was purchased from Biomeda (CA, U.S.A.).

Results

Ultrastructural study

In order to confirm that $Cav1^{-/-}$ mice lacked caveolae in their small intestinal smooth muscles, ultrastructural examination of the longitudinal muscles was carried out using the electron microscope. Previous work in our laboratory has demonstrated that ICC and smooth muscles of mouse intestine contain a large number of caveolae that typically appeared in the electron microscope images as flask-shaped invaginations of the plasma membrane (Daniel *et al*., 2004). However, electron microscope imaging of the longitudinal muscle cells in $Cav1^{-/-}$ mouse intestine revealed total loss of caveolae on the plasma membrane of these cells (Figure 1b). The absence of caveolar structures was very evident upon comparison with the electron microscope image of the longitudinal muscle cells in the control mice (Figure 1a).

Immunohistochemical studies

Double immunohistochemical staining in cryosections Cryosections stained with caveolin-1 antibody and the antibody for nNOS with COOH-terminal epitope, which recognizes the myogenic variant of nNOS (Daniel *et al*., 2001), showed lack of both caveolin-1 and nNOS-C in the smooth muscle cells and ICC of $Cav1^{-/-}$ mice (Figure 2a–c). Our laboratory showed previously that nNOS-C is closely co-localized with caveolin-1 at punctate sites in the cell periphery of circular and longitudinal muscle cells of BALB/c mice (Cho & Daniel, 2005).

Cryosections stained with caveolin-1 antibody and antibody for nNOS with NH_2-terminal epitope (nNOS-N), which recognizes the nerve-resident variant of nNOS in myenteric plexus (Cho & Daniel, 2005), also showed loss of caveolin-1 immunoreactivity in $Cav1^{-/-}$ mice compared to control mice. However, nNOS-N-specific immunoreactivity was comparable and showed a cytoplasmic localization in myenteric neurons (data not shown).

Single immunohistochemical staining in whole-mount preparations To examine the presence and distribution of myenteric plexus ICC, single staining with anti-vimentin, which recognizes vimentin filaments characteristically present in the ICC (Komuro *et al*., 1999), of whole-mount preparations of the jejunal tissue in $Cav1^{+/+}$ and $Cav1^{-/-}$ was carried out. Anti-vimentin was used to stain ICC in the small intestine of mouse (Fujita *et al*., 2003) and other species (Torihashi *et al*., 1993; Ishikawa & Komuro, 1996; Andries *et al*., 2000). It showed that the myenteric plexus ICC were equally present

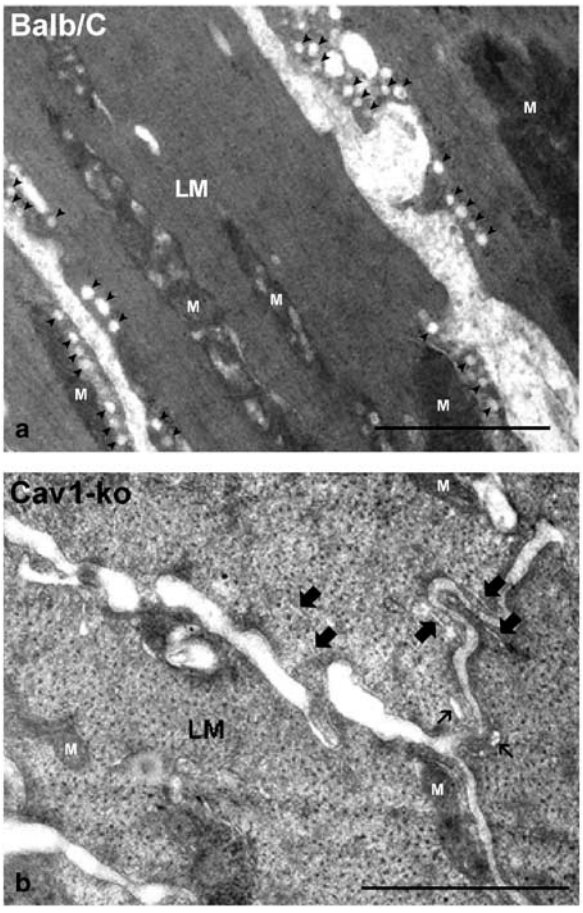

Figure 1 An electron microscope image of the longitudinal muscle layer (LM) of mouse small intestine. Note the total absence of the flask-shaped caveolae on the plasma membrane of the longitudinal muscle cells of $Cav1^{-/-}$ (b) as compared to the longitudinal muscle cells of the control BALB/c mouse (a). Caveolae are indicated by solid arrowheads. Small endoplasmic reticulum profiles (marked with thick arrows) and sarcoplasmic reticulum (marked with thin arrows) remain. Mitochondria are labeled with (M). $Cav1^{+/+}$ intestine showed similar caveolae profile to the BALB/c (data not shown). Length bars are 1 μm.

and similarly distributed in the small intestine of $Cav1^{+/+}$ and $Cav1^{-/-}$ strains (Figure 2d and e).

Double immunohistochemical staining in whole-mount preparations This technique was used to quantify the differences in expression of nNOS-N in the myenteric neurons in $Cav1^{-/-}$ and $Cav1^{+/+}$ mice (Figure 2f–k). The number of cells showing specific staining with human neuronal protein HuC/D antibody, which recognizes the cytoplasm and the nucleus of myenteric neurons (Lin *et al*., 2002; Chiocchetti *et al*., 2004), was considered to be the total number of myenteric neurons. The percentage of myenteric neurons expressing nNOS-N was determined in the myenteric ganglia of $Cav1^{+/+}$ and $Cav1^{-/-}$ mice. The number of myenteric plexus ganglia examined was eight in $Cav1^{+/+}$ and 13 in $Cav1^{-/-}$. Out of a total of 123 nerve cells examined in $Cav1^{-/-}$, 78.9% showed nNOS-N IR, while only 63.1% out of 84 nerve cells showed nNOS-N IR in $Cav1^{+/+}$ myenteric ganglia. The results indicate an increase in the percentage of myenteric neurons expressing nNOS-N in $Cav1^{-/-}$ (two-sided P-value = 0.0172).

Functional studies

Spontaneous activity The amplitudes of the spontaneous muscle contractions in $Cav1^{-/-}$ and the control species were measured at the mid-point of the equilibration period. The values in mg tension are: 199.38 ± 34.19 for BALB/c ($n = 13$), 160 ± 23.53 for $Cav1^{+/+}$ ($n = 10$), and 182.82 ± 21.89 for $Cav1^{-/-}$ ($n = 17$). Statistical analysis showed that there were no significant differences between the amplitudes of the spontaneous contractions in the three mice strains. There was no significant difference between the values measured from the ileum and the jejunum in a single mouse strain.

Effects of LNNA on EFS-induced relaxations EFS in NANC conditions elicited a transient relaxation, which increased in magnitude as the stimulation frequency was increased to reach a maximum at 10 pps. All three strains showed relaxations of comparable magnitudes (no significant differences). In both control strains, inhibiting NOS function with 100 μM LNNA abolished EFS-evoked relaxations at all stimulation frequencies (Figure 3a, b). On the contrary, in $Cav1^{-/-}$, LNNA only reduced the relaxations at 1 and 3 pps stimulations and had no significant effect on the relaxations at 10 and 30 pps (Figure 3c). The responses to EFS and the effects of LNNA were similar in tissue segments obtained from the ileum and the jejunum in the same mouse strain (data not shown).

Responses to SNP SNP (100 μM), which acts by generating NO, produced a reduction in the amplitude of contractions and an inhibition of the phasic activity of the muscle. The magnitudes of SNP-induced inhibitions were greater in control mice compared to $Cav1^{-/-}$ mice (Figure 4). The effects of SNP were similar in tissue segments obtained from the ileum and jejunum in the same mouse strain (data not shown).

Responses to BCGMP BCGMP (100 μM), a plasma-membrane permeable analogue of the second messenger cyclic guanosine monophosphate (cGMP), produced a reduction in the amplitude of contraction of the muscle. There were no significant differences among the magnitudes of BCGMP-induced inhibitions in $Cav1^{-/-}$ mice and the control mice (Figure 5). The effects of BCGMP were similar in tissue segments obtained from the ileum and jejunum in the same mouse strain (data not shown).

Effects of apamin on EFS-induced relaxations Apamin (1 μM), which acts by blocking a small-conductance Ca^{2+}-dependant K^+ channel (Matsuda *et al*., 2004), caused a significant reduction in the magnitudes of EFS-induced relaxations at all stimulation frequencies in $Cav1^{-/-}$ mice (Figure 6a). In $Cav1^{+/+}$ control mice, the effect of apamin on the magnitude of EFS-induced relaxation was smaller and more variable, causing it to be statistically insignificant, except at the stimulation frequency of 30 pps (Figure 6b). The effect of apamin was similar in tissue segments obtained from the ileum and jejunum in the same mouse strain (data not shown). In the experiments in $Cav1^{-/-}$ where LNNA was added after the first cycle of EFS, it was found that the combination of

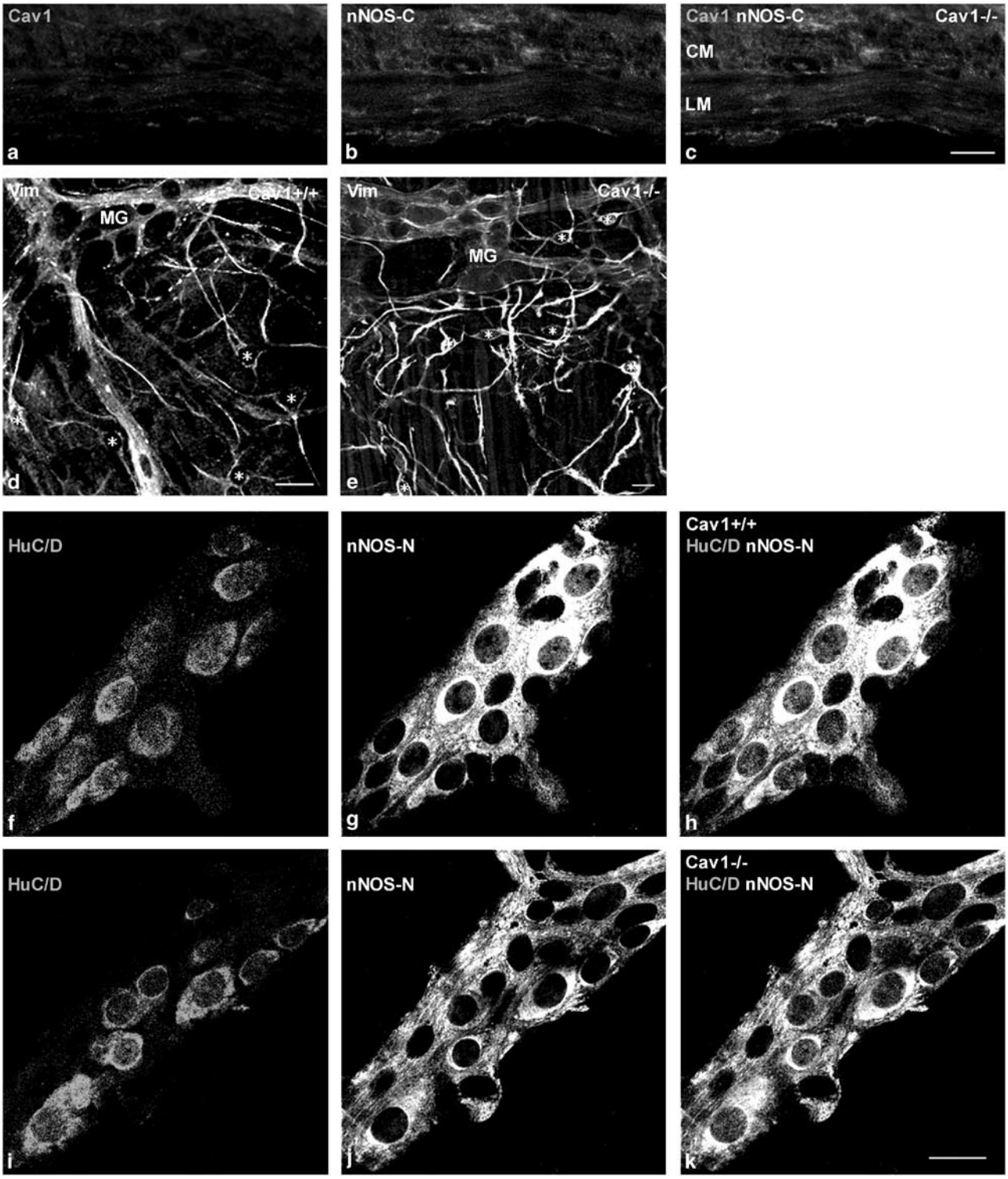

Figure 2 Immunohistochemical staining of cryosections from $Cav1^{-/-}$ jejunum (a–c) and whole-mount preparations of myenteric plexus layer from $Cav1^{+/+}$ and $Cav1^{-/-}$ jejunal tissues (d–k). Panels (a)–(c) show that there are no caveolin-1 and nNOS-C-immunoreactivities in all ICC and smooth muscles layers of $Cav1^{-/-}$ jejunum. Panels (d) and (e) show myenteric ICC stained with anti-vimentin in $Cav1^{+/+}$ and $Cav1^{-/-}$ myenteric plexus, respectively. ICCs are marked with asterisks. Note that the myenteric plexus ICC are equally present and similarly distributed in both strains. Panels (f)–(k) show double staining of whole-mount preparations for myenteric neurons HuC/D protein and nNOS-N. Panels (f) and (i) show myenteric neurons stained with HuC/D in $Cav1^{+/+}$ and $Cav1^{-/-}$ myenteric plexus, respectively. Panels (g) and (j) show myenteric neurons and nerve fibers stained with nNOS-N in $Cav1^{+/+}$ and $Cav1^{-/-}$ myenteric plexus, respectively. Panels (h) and (k) show myenteric neurons co-localized with HuC/D and nNOS-N in $Cav1^{+/+}$ and $Cav1^{-/-}$ myenteric plexus, respectively. Note the persistence of nNOS-N in myenteric neurons in $Cav1^{-/-}$ intestine. Length bars are 20 μm for panels (a)–(c), (d) and (e), and (f)–(k).

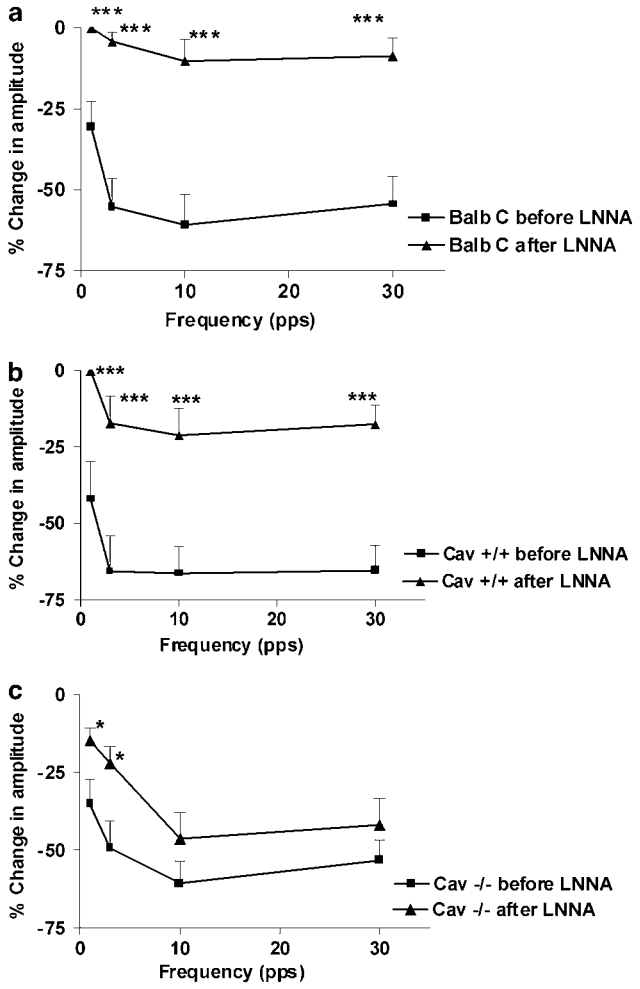

Figure 3 Effect of LNNA (100 μM) on the inhibitory responses obtained by EFS in NANC conditions at different stimulation frequencies (0.5 ms, 50 V cm^{-1} for 10 s). The magnitudes of the EFS-evoked responses are expressed as the % change in the amplitude (the amplitude of the inhibitory phase normalized to the amplitude of the muscle activity directly precedent to the inhibitory stimulus) and the values shown are mean$\pm$s.e. (a, b) LNNA abolishes the EFS-induced inhibitions at all frequencies in BALB/c and Cav1$^{+/+}$, respectively. Significance is tested by ANOVA followed by Bonferroni's test (***$P<0.001$, n-value = 7 for BALB/c and 6 for Cav1$^{+/+}$). (c) LNNA significantly reduces the EFS-induced inhibitions only at 1 and 3 pps (*$P<0.05$, n-value = 11), and had no effect on the inhibitions at 10 and 30 pps in Cav$^{-/-}$ mice.

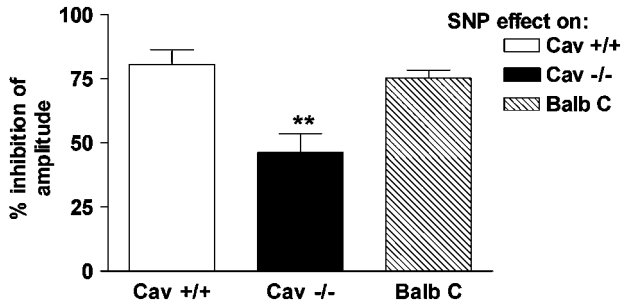

Figure 4 The inhibitory effect produced by 100 μM SNP on longitudinal muscle preparations from the small intestine of Cav1$^{+/+}$, Cav1$^{-/-}$, and BALB/c mice. The inhibitory effects were more pronounced in wild-type mice compared to Cav1$^{-/-}$. The magnitudes of inhibition are expressed as the % inhibition of the amplitude (amplitude of the inhibitory phase normalized to the amplitude of the muscle activity directly precedent to the addition of SNP). The values are shown as mean$\pm$s.e. of six experiments. Significance was tested by ANOVA, followed by Bonferroni test (**$P<0.01$).

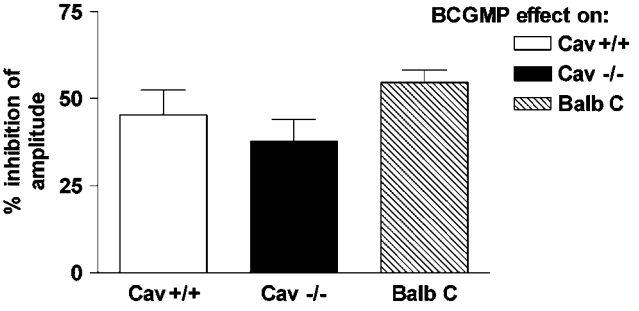

Figure 5 The inhibitory effect produced by 100 μM BCGMP on longitudinal muscle preparations from the small intestine of Cav1$^{+/+}$, Cav1$^{-/-}$, and BALB/c mice. There were no significant differences among the magnitudes of inhibition, which are expressed as the % inhibition of the amplitude (amplitude of the contractions 5 min after the addition of BCGMP normalized to the amplitude of the muscle contraction directly precedent to its addition). The values shown are mean$\pm$s.e. of six experiments. Significance was tested by ANOVA, followed by Bonferroni test.

LNNA and apamin abolished the EFS-evoked relaxation at 1 and 3 pps. However, residual inhibitions of -15.99 ± 3.03 and -22.27 ± 4.06% persisted at 10 and 30 pps, respectively ($n=6$). This effect was similar in both the ileum and the jejunum of the Cav1$^{-/-}$ strain.

Discussion and conclusions

Caveolin-1 is known to exert regulatory effects on the different NOS isoforms, which normally reside in the caveolae (Feron *et al*., 1996). The present study examined the possible role of caveolin-1 in the regulation of NO function in the mouse small intestine. Ultrastructural examination of the longitudinal smooth muscles of Cav1$^{-/-}$ small intestine confirmed the absence of caveolae. In addition, caveolin-1, as well as the associated protein (Cho & Daniel, 2005), nNOS-C, was absent in the smooth muscles and ICC in small intestine of Cav1$^{-/-}$ mice.

Previous work carried out on *mdx* mice, that lack dystrophin due to an X-linked mutation (Bulfield *et al*., 1984), showed defective NO production in the colon (Mulè *et al*., 2001) in addition to a reduction in the responsiveness to EFS in NANC conditions and to SNP in the duodenum (Zizzo *et al*., 2003). Dystrophin anchors nNOS at the inner surface of the sarcolemma in skeletal muscle fibers (Brenman *et al*., 1995). Both dystrophin and caveolin-3, the striated muscle analogue of caveolin-1 (Razani *et al*., 2002), co-immunoprecipitate and interact with β-dystroglycan (Sotgia *et al*., 2000). This relationship between dystrophin and caveolin-1, together with our observations, suggests a possible functional defect in NO function in the Cav1$^{-/-}$ intestine similar to that in the *mdx* intestine.

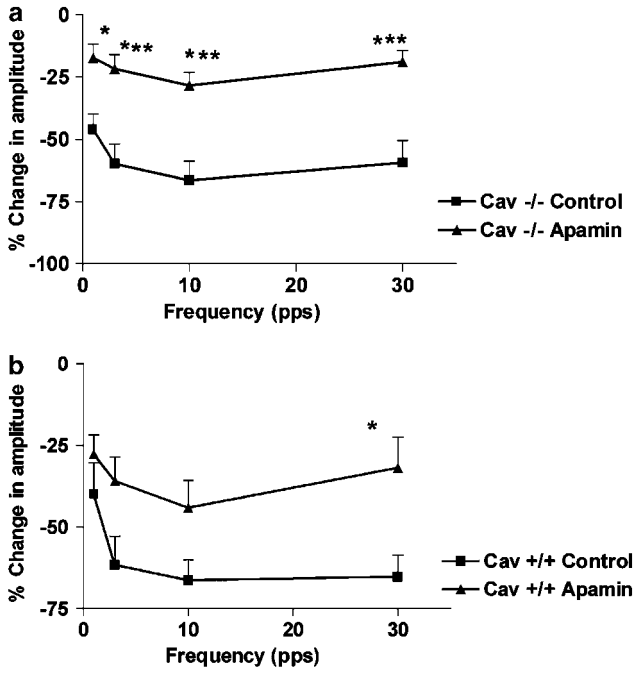

Figure 6 Effect of apamin (1 μM) on the inhibitory responses induced by EFS in the NANC conditions at different stimulation frequencies (0.5 ms, 50 V cm^{-1} for 10 s). The magnitudes of the EFS-evoked responses are expressed as the % change in the amplitude (the amplitude of the inhibitory phase normalized to the amplitude of the muscle activity directly precedent to the inhibitory stimulus), and the values shown are mean $\pm$ s.e. (a) Apamin significantly reduced the magnitude of EFS-induced inhibitions at all frequencies in Cav1$^{-/-}$ mouse intestine. Significance was tested by ANOVA, followed by Bonferroni test (*$P<0.05$; ***$P<0.001$, n-value = 6). (b) Apamin did not produce a significant effect on the EFS-induced inhibitions in the Cav1$^{+/+}$ mouse intestine, except at 30 pps (*$P<0.05$, n-value = 6).

To test this hypothesis, the effect of block of NO synthesis by LNNA on EFS-induced relaxations in NANC conditions in small intestinal smooth muscles was studied. LNNA attenuated EFS-evoked relaxations much less in Cav1$^{-/-}$ tissues, suggesting that NO played a lesser functional role in these tissues. However, immunohistochemical staining for nNOS-N, the nerve-resident variant, indicated that Cav1$^{-/-}$ myenteric neurons containing nNOS were still present in myenteric ganglia. The persistence of nNOS-N may be due to the fact that it is a different splice variant and has a cytoplasmic localization in nerves (Salapatek *et al*., 1998b) and that nerves lack any detectable caveolin-1 (Wu *et al*., 1997). This finding ruled out the suggestion that the reduced NO function was due to a decrease in sources of nNOS; that is, the myenteric neurons expressing nNOS-N. In addition, these findings are consistent with similar studies in *mdx* mouse, where nNOS was spared in myenteric neurons from the colon (Mulè *et al*., 2001).

To determine whether the cause of the defective NO function in the Cav1$^{-/-}$ mouse small intestine was post-junctional or pre-junctional, we examined the effects of SNP, a source of exogenous NO (Zizzo *et al*., 2003), on smooth muscle contraction. Cav1$^{-/-}$ preparations showed reduced responsiveness to SNP compared to control (BALB/c and Cav1$^{+/+}$) preparations. This was not due to a general failure to relax, since relaxation of segments from Cav1$^{-/-}$ mice to EFS was comparable to that from control segments; that is, EFS-induced inhibition was just less sensitive to LNNA and more sensitive to apamin. Consequently, we suggest that post-junctional abnormalities occur in ICC and/or smooth muscles, leading to the impaired response to NO. Also, it is more likely a deficiency at some point in the intracellular signal transduction cascade than a nerve-to-muscle signal transmission abnormality, since nNOS is expressed in the myenteric neurons from Cav1$^{-/-}$ mice.

To determine the level of the deficiency downstream of the NO signal, the inhibitory responses to BCGMP, the plasma membrane-permeable analogue of cGMP (Zizzo *et al*., 2003), the second messenger usually generated by NO stimulation, were compared in all three strains. The absence of significant differences between the Cav1$^{-/-}$ and the control strains indicates that the deficiency lies before the level of cGMP-controlled effectors. This might be due to a decrease in soluble guanylyl cyclase; yet this hypothesis and other possible mechanisms still require further experimentation. Nevertheless, the absence of nNOS-C provides a clear example of the structural abnormalities imparted by caveolin-1 gene knockout in small intestinal smooth muscles and ICC, which are well known to play a crucial role in nerve-to-muscle signal transmission in the gastrointestinal tract (Sanders, 1996). Moreover, the increase in the number of myenteric nerve cells expressing nNOS in Cav1$^{-/-}$ mice, seen upon quantification of the immunohistochemical staining results in whole-mount preparations, might be a possible compensatory outcome of the reduced muscle and ICC NO responsiveness. In addition, this observation provides further evidence that the impairment of NO function is most likely to be post-junctional.

Despite reduced responses to NO, EFS produced relaxations in the Cav1$^{-/-}$ small intestine that were comparable in magnitude to those obtained in the control mouse small intestine. This suggests that the relaxing function of NO in the Cav1$^{-/-}$ small intestine was substituted by other mediators. ATP is an established inhibitory neurotransmitter (Bauer & Matusak, 1986) that elicits inhibitory responses due to the activation of small-conductance Ca^{2+}-dependant K^+-channels (Ohno *et al*., 1996). Moreover, the pituitary adenylate cyclase-activating peptide (PACAP) is a neurotransmitter that induces inhibitory effects in different gastrointestinal segments from several animal species (Kishi *et al*., 1996; Chakder & Rattan, 1998; Pluja *et al*., 2000). This inhibitory effect might be due to the opening of apamin-sensitive K^+-channels (Pluja *et al*., 2000). PACAP has recently been reported to act directly on the smooth muscles of the mouse small intestine (Zizzo *et al*., 2004). Therefore, addition of apamin may have affected both ATP and PACAP functions in the Cav1$^{-/-}$ and the Cav1$^{+/+}$ small intestine. Apamin-induced reduction in EFS-evoked relaxations was only significant in Cav1$^{-/-}$ intestine. This finding points out the fact that the contribution of apamin-sensitive inhibitory mediators to the regulation of Cav1$^{-/-}$ small intestine motility increases in importance, possibly to compensate for the reduced NO function. However, these might not be the only possible mechanisms involved in the inhibitory neurotransmission in the Cav1$^{-/-}$ small intestine. This was evident when a combination of apamin and LNNA was used, since residual inhibition of the amplitude of the contractions persisted at 10 and 30 pps. These results agree with other published data, where a combination of LNNA and apamin only reduced the amplitudes of EFS-evoked inhibitory junction potentials by 50% in mouse colon

(Spencer *et al*., 1998b). Vasoactive intestinal peptide (VIP) is one of the important mediators that could likely be involved in this residual inhibition, since the complete co-localization between NOS and VIP in mouse small intestine nerves has been reported (Sang & Young, 1996). However, further research is required to verify and elucidate the nature of the involved mediator(s).

In conclusion, the current study shows that caveolin-1 is necessary for normal NO function in the mouse intestine. Caveolin-1 gene knockout causes abnormalities in the ICC and smooth muscles of the mouse intestine, leading to a reduced responsiveness to endogenous and exogenous NO. The impairment of NO function in $Cav1^{-/-}$ mouse intestine may be compensated by the apamin-sensitive inhibitory mediators.

This research was supported by the Canadian Institute for Health Research (CIHR).

References

ANDRIES, L., DUYMELINCK, C. & BORGERS, M. (2000). Muscle and non-muscle markers in the interstitial cells of Cajal of guinea pig small intestine and colon. *Gastroenterology,* **118,** A4819 (abstract).

AZZENA, G.B. & MANCINELLI, R. (1999). Nitric oxide regenerates the normal colonic peristaltic activity in *mdx* dystrophic mouse. *Neurosci. Lett.,* **261,** 9–12.

BAUER, V. & MATUSAK, O. (1986). The non-adrenergic non-cholinergic innervation in the small intestine. *Arch. Int. Pharmacodyn. Ther.,* **280,** 137–163.

BRENMAN, J.E., CHAO, D.S., XIA, H., ALDAPE, K. & BREDT, D.S. (1995). Nitric oxide synthase complexed with dystrophin and absent from skeletal muscle sarcolemma in Duchenne muscle dystrophy. *Cell,* **82,** 743–752.

BUCCI, M., GRATTON, J.-P., RUDIC, R.D., ACEVEDO, L., ROVIEZZO, F., CIRINO, G. & SESSA, W.C. (2000). *In vivo* delivery of caveolin-1 scaffolding domain inhibits nitric oxide synthesis and reduces inflammation. *Nat. Med.,* **6,** 1362–1367.

BULFIELD, G., SILLER, W.G., WIGHT, P.A. & MOORE, K.J. (1984). X chromosome-linked muscular dystrophy (mdx) in the mouse. *Proc. Natl. Acad. Sci. U.S.A.,* **81,** 1189–1192.

CHAKDER, S. & RATTAN, S. (1998). Involvement of pituitary adenylate cyclase-activating peptide in opossum internal anal sphincter relaxation. *Am. J. Physiol.,* **275,** G769–G777.

CHANG, W.J., YING, Y., ROTHBERG, K., HOOPER, N., TURNER, A., GAMBLIEL, H., DE GUNZBERG, J., MUMBY, S., GILMAN, A. & ANDERSON, R. (1994). Purification and characterization of smooth muscle cell caveolae. *J. Cell Biol.,* **126,** 127–138.

CHIOCCHETTI, R., GRANDIS, A., BOMBARDI, C., CLAVENZANI, P., COSTERBOSA, G.L., LUCCHI, M.L. & FURNESS, J.B. (2004). Characterisation of neurons expressing calbindin immunoreactivity in the ileum of the unweaned and mature sheep. *Cell Tissue Res.,* **318,** 289–303.

CHO, W.J. & DANIEL, E. (2005). Proteins of interstitial cells of Cajal and intestinal smooth muscle, co-localized with caveolin-1. *Am. J. Physiol. Gastrointest. Liver Physiol.,* **288,** G571–G585.

COUET, J., LI, S., OKAMOTO, T., IKEZU, T. & LISANTI, M.P. (1997). Identification of peptide and protein ligands for the caveolin-scaffolding domain. Implications for the interaction of caveolin with caveolae-associated proteins. *J. Biol. Chem.,* **272,** 6525–6533.

DANIEL, E., BODIE, G., MANNARINO, M., BODDY, G. & CHO, W.J. (2004). Changes in membrane cholesterol affect caveolin-1 localization and ICC-pacing in mouse jejunum. *Am. J. Physiol. Gastrointest. Liver Physiol.,* **287,** G202–G210.

DANIEL, E., JURY, J. & WANG, Y.F. (2001). nNOS in canine lower esophageal sphincter: co-localized with caveolin-1 and Ca^{2+}-handling proteins? *Am. J. Physiol. Gastrointest. Liver Physiol.,* **281,** G1101–G1114.

DRAB, M., VERKADE, P., ELGER, M., KASPER, M., LOHN, M., LAUTERBACH, B., MENNE, J., LINDSCHAU, C., MENDE, F. & LUFT, F.C. (2001). Loss of caveolae, vascular dysfunction and pulmonary defects in Caveolin-1 gene disrupted mice. *Science,* **293,** 2449–2452.

ENGLEMAN, J.A., ZHANG, X.L., GALBIATI, F., VOLONTE, D., SOTGIA, F., PESTELL, R.G., MINETTI, C., SCHERER, P.E., OKAMOTO, T. & LISANTI, M.P. (1998). Molecular genetics of the caveolin gene family: implications for human cancer, diabetes, Alzheimer's disease and muscle dystrophy. *Am. J. Hum. Genet.,* **63,** 1578–1587.

FELLY-BOSCO, E., BENDER, F.C., COURJAULT-GAUTIER, F., BRON, C. & QUEST, A. (2000). Caveolin-1 down-regulates inducible nitric oxide synthase *via* the proteasome pathway in human colon carcinoma cells. *Proc. Natl. Acad. Sci. U.S.A.,* **97,** 14334–14339.

FERON, O., BELHASSEN, L., KOBZIK, L., SMITH, T.W., KELLY, R.A. & MICHEL, T. (1996). Endothelial nitric oxide synthase targeting to caveolae. Specific interactions with caveolin isoforms in cardiac myocytes and endothelial cells. *J. Biol. Chem.,* **271,** 22810–22814.

FUJITA, A., TAKEUCHI, T., JUN, H. & HATA, F. (2003). Localization of Ca^{2+}-activated K^+-channel, SK3, in fibroblast-like cells forming gap junctions with smooth muscle cells in the mouse small intestine. *J. Pharmacol. Sci.,* **92,** 35–42.

GARCIA-CARDENA, G., FAN, R., STERN D.F. LIU, J. & SESSA, W.C. (1996a). Endothelial nitric oxide synthase is regulated by tyrosine phosphorylation and interacts with caveolin-1. *J. Biol. Chem.,* **271,** 27237–27240.

GARCIA-CARDENA, G., MARTASEK, P., MASTERS, B., SKIDD, P.M., COUET, J., LI, S., LISANTI, M.P. & SESSA, W.C. (1997). Dissecting the interaction between nitric oxide synthase (NOS) and caveolin. Functional significance of the NOS caveolin binding domain *in vivo*. *J. Biol. Chem.,* **272,** 25437–25440.

GARCIA-CARDENA, G., OH, P., LIU, J., SCHNITZER, J. & SESSA, W.C. (1996b). Targeting of nitric oxide synthase to endothelial cell caveolae *via* palmitoylation: implications for nitric oxide signaling. *Proc. Natl. Acad. Sci. U.S.A.,* **93,** 6448–6453.

HUBER, A., SAUR, D., KURJAK, M., SCHUSDZIARRA, V. & ALLESCHER, H.D. (1998). Characterization and splice variants of neuronal nitric oxide synthase in small intestine. *Am. J. Physiol. Gastrointest. Liver Physiol.,* **275,** G1146–G1156.

ISHIKAWA, K. & KOMURO, T. (1996). Characterization of the interstitial cells associated with the sub-muscular plexus of the guinea pig colon. *Anat. Embryol. (Berlin),* **194,** 49–55.

JU, H., ZOU, R., VENEMA, V.J. & VENEMA, R.C. (1997). Direct interaction of endothelial nitric-oxide synthase and caveolin-1 inhibits synthase activity. *J. Biol. Chem.,* **272,** 18522–18525.

KISHI, K., TAKEUCHI, T., SUTHAMNATPONG, N., NISHIO, T. & HATA, F. (1996). VIP and PACAP mediate non-adrenergic non-cholinergic inhibition in longitudinal muscle of rat distal colon: involvement of activation of charybdotoxin- and apamin-sensitive K^+ channels. *Br. J. Pharmacol.,* **119,** 623–630.

KOMURO, T., SEKI, K. & HORIGUCHI, K. (1999). Ultrastructural characterization of the interstitial cells of Cajal. *Arch. Histol. Cytol.,* **62,** 295–316.

LIN, Z., GAO, N., HU, H.-Z., LIU, S., GAO, C., KIM, G., REN, J., XIA, Y., PECK, O.C. & WOOD, J.D. (2002). Immunoreactivity of Hu proteins facilitates the identification of myenteric neurones in guinea pig small intestine. *Neurogastroenterol. Motil.,* **14,** 197–204.

LYSTER, D.J., BYWATER, R.A. & TAYLOR, G.S. (1995). Neurogenic control of myoelectric complexes in the mouse isolated colon. *Gastroenterology,* **108,** 1371–1378.

MATSUDA, N.M., MILLER, S.M., SHA, L., FARRUGIA, G. & SZURSZEWSKI, J.H. (2004). Mediators of non-adrenergic non-cholinergic inhibitory neurotransmission in porcine jejunum. *Neurogastroenterol. Motil.,* **16,** 605–611.

MICHEL, J., FERON, O., SACKS, D. & MICHEL, T. (1997). Reciprocal regulation of endothelial nitric-oxide synthase by Ca^{2+}-calmodulin and caveolin. *J. Biol. Chem.,* **272,** 15583–15586.

MULÈ, F. & SERIO, R. (2002). Spontaneous mechanical activity and evoked responses in isolated gastric preparations in normal and dystrophic (*mdx*) mice. *Neurogastroenterol. Motil.,* **14,** 667–676.

MULÈ, F., D'ANGELO, S., TABACCHI, G., AMATO, A. & SERIO, R. (1999). Mechanical activity in small and large intestine in normal and *mdx* mice: a comparative analysis. *Nerogastroenterol. Motil.,* **11,** 133–139.

MULÈ, F., VANNUCHI, M.G., CORSANI, L., SERIO, R. & FAUSSONE-PELLEGRINI, M.S. (2001). Myogenic NOS and endogenous NO production are defective in colon from dystrophic (*mdx*) mice. *Am. J. Physiol. Gastrointest. Liver Physiol.,* **281,** G1264–G1270.

OHNO, N., XUE, L., YAMAMOTO, Y. & SUZUKI, H. (1996). Properties of the inhibitory junction potential in smooth muscle of the guinea pig gastric fundus. *Br. J. Pharmacol.,* **117,** 974–978.

OKAMOTO, T., SCHLEGEL, A., SCHERER, P.E. & LISANTI, M.P. (1998). Caveolins: a family of scaffolding proteins for organizing 'pre-assembled signaling complexes' at the plasma membrane. *J. Biol. Chem.,* **273,** 5419–5422.

OKASORA, T., BYWATER, R.A. & TAYLOR, G.S. (1986). Projections of enteric motor neurons in the mouse distal colon. *Gastroenterology,* **90,** 1964–1971.

PLUJA, L., FERNANDEZ, E. & JIMENEZ, M. (2000). Electrical and mechanical effects of vasoactive intestinal peptide and pituitary adenylate cyclase-activating peptide in the rat colon involve different mechanisms. *Eur. J. Pharmacol.,* **389,** 217–224.

RAZANI, B., ENGLEMAN, J.A., WANG, X.B., SCHUBERT, W., ZHANG, X.L., MARKS, C.B., MACALUSO, F., RUSSEL, R.G., LI, M. & PESTELL, R.G. (2001). Caveolin-1 null mice are viable, but show evidence of hyper-proliferative and vascular abnormalities. *J. Biol. Chem.,* **276,** 38121–38138.

RAZANI, B., WOODMAN, S. & LISANTI, M. (2002). Caveolae: from cell biology to animal physiology. *Pharmacol. Rev.,* **54,** 431–467.

ROTHBERG, K., HEUSER, J., DONZELL, W., YING, Y., GLENNY, J.R. & ANDERSON, R.G.W. (1992). Caveolin, a protein component of caveolae membrane coats. *Cell,* **68,** 673–682.

SALAPATEK, A.M., WANG, W.F., MAO, Y.K., MORI, M. & DANIEL, E. (1998a). Myogenic NOS in canine lower esophageal sphincter: enzyme activation, substrate recycling and product actions. *Am. J. Physiol. Cell. Physiol.,* **274,** C1145–C1157.

SALAPATEK, A.M., WANG, Y.F., MAO, Y.K., LAM, A. & DANIEL, E. (1998b). Myogenic nitric oxide synthase activity in lower canine lower osophageal sphincter: morphological and functional evidence. *Br. J. Pharmacol.,* **123,** 1055–1064.

SANDERS, K.M. (1996). A case for interstitial cells of Cajal as pacemakers and mediators of neurotransmission in the gastrointestinal tract. *Gastroenterology,* **111,** 492–515.

SANG, Q. & YOUNG, H.M. (1996). The identification and chemical coding of cholinergic neurons in the small and large intestine of the mouse. *Cell Tissue Res.,* **284,** 39–53.

SARGIACOMO, M., SCHERE, P.E., TANG, Z., KUBLER, E., SONGS, K.S., SANDERS, M.C. & LISANTI, M.P. (1995). Oligomeric structure of caveolin: implications for caveolae membrane organization. *Proc. Natl. Acad. Sci. U.S.A.,* **92,** 9407–9411.

SATO, Y., IKUKO, S. & SHIMIZU, T. (2004). Identification of caveolin-1-interating site in neuronal nitric-oxide synthase. *J. Biol. Chem.,* **279,** 8827–8836.

SATOH, Y., TAKEUCHI, T. & YAMAZAKI, Y. (1999). Mediators of nonadrenergic, noncholinergic relaxation in longitudinal muscle of the ICR mice. *J. Smooth Muscle Res.,* **35,** 65–75.

SCHERER, P.E., LISANTI, M.P., BALDINI, G., SARGIACOMO, M., CORLEY-MASTICK, C. & LODISH, H.F. (1994). Induction of caveolin during adipogenesis and association of GLUT4 with caveolin-rich vesicles. *J. Cell Biol.,* **127,** 1233–1243.

SCHERER, P.E., TANG, Z., CHAN, M., SARGIACOMO, M., LODISH, H.F. & LISANTI, M.P. (1995). Caveolin isoforms differ in their N-terminal protein sequence and subcellular distribution. *J. Biol. Chem.,* **270,** 16395–16401.

SEGAL, S.S., BRETT, S.E. & SESSA, W.C. (1999). Codistribution of NOS and caveolin throughout peripheral vasculature and skeletal muscles of hamsters. *Am. J. Physiol.,* **277,** H1167–H1177.

SERIO, R., BONVISSUTO, F. & MULE, F. (2001). Altered electrical activity in colonic smooth muscle cells from dystrophic (*mdx*) mice. *Neurogastroenterol. Motil.,* **13,** 169–175.

SMART, E.J., GRAF, G.A., MCNIVEN, M.A., SESSA, W.C., ENGLEMAN, J.A., SCHERER, P.E., OKAMOTO, T. & LISANTI, M.P. (1999). Caveolins: liquid-ordered domains and signal transduction. *Mol. Cell. Biol.,* **19,** 7289–7304.

SOTGIA, F., LEE, J.K., DAS, K., BEDFORD, M., PETRUCCI, T.C., MACIOCE, P., SARGIACOMO, M., BRICARELLI, F.D., MINETTI, C., SUDOL, M. & LISANTI, M.P. (2000). Caveolin-3 directly interacts with the C-terminal tail of beta-dystroglycan. Identification of a central WW-like domain within caveolin family members. *J. Biol. Chem.,* **275,** 38048–38058.

SOTGIA, F., RAZANI, B., BONUCCELLI, G., SCHUBERT, W., BATTISTA, M., LEE, H., CAPOZZA, F., SCHUBERT, A.L., MINETTI, C., BUCKLEY, J.T. & LISANTI, M.P. (2002). Intracellular retention of glycosylphosphatidyl inositol-linked proteins in caveolin-deficient cells. *Mol. Cell. Biol.,* **22,** 3905–3926.

SPENCER, N.J., BYWATER, R.A., HOLMAN, M.E. & TAYLOR, G.S. (1998b). Spontaneous and evoked inhibitory junction potentials in the circular muscle layer of the mouse colon. *J. Auton. Nerv. Syst.,* **69,** 115–121.

SPENCER, N.J., BYWATER, R.A. & TAYLOR, G.S. (1998a). Disinhibition during myoelectric complexes in mouse colon. *J. Auton. Nerv. Syst.,* **71,** 37–47.

TANG, Z.-L., SCHERER, P.E., OKAMOTO, T., SONG, K., CHU, C., KOHTZ, D.S., NISHIMOTO, I., LODISH, H.F. & LISANTI, M.P. (1996). Molecular cloning of caveolin-3, a novel member of the caveolin gene family expressed predominantly in muscle. *J. Biol. Chem.,* **271,** 2255–2261.

TORIHASHI, S., KOBAYASHI, S., GERTHOFFER, W.T. & SANDERS, K.M. (1993). Interstitial cells in deep muscular plexus of canine small intestine may be specialized smooth muscle cells. *Am. J. Physiol.,* **265,** G638–G645.

VENEMA, V.J., JU, H., ZOU, R. & VENEMA, R.C. (1997). Interaction of neuronal nitric-oxide synthase with caveolin-3 in skeletal muscle. Identification of a novel caveolin scaffolding/inhibitory domain. *J. Biol. Chem.,* **272,** 28187–28190.

WU, C., BUTZ, S., YING, Y.-S. & ANDERSON, R.G.W. (1997). Tyrosine kinase receptors concentrated in caveolae-like domains from neuronal plasma membrane. *J. Biol. Chem.,* **272,** 3554–3559.

ZIZZO, M.G., MULE, F. & SERIO, R. (2003). Duodenal contractile activity in dystrophic (*mdx*) mice: reduction of nitric oxide influence. *Neurogastroenterol. Motil.,* **15,** 559–565.

ZIZZO, M.G., MULE, F. & SERIO, R. (2004). Interplay between PACAP and NO in mouse ileum. *Neuropharmacology,* **46,** 449–455.

(Received February 15, 2005
Revised April 15, 2005
Accepted April 26, 2005
Published online 6 June 2005)